INTERFACE

royalsocietypublishing.org/journal/rsif

Research

Cite this article: Griffin BW, Prescott TL, Jannel A, Falkingham PL. 2026 Penetrative track morphology and sediment parameters: subsurface layers are robust to changes in substrate properties. *J. R. Soc. Interface* **23**: 20250796.
https://doi.org/10.1098/rsif.2025.0796

Received: 1 August 2025
Accepted: 2 December 2025

Subject Category:
Life Sciences–Earth Science interface

Subject Areas:
biomechanics

Keywords:
footprint, fossil, dinosaur, bird, discrete element modelling, undertracks

Author for correspondence:
Benjamin William Griffin
e-mails: B.W.Griffin@ljmu.ac.uk; ben.pterosaur@gmail.com

Electronic supplementary material is available online at https://doi.org/10.6084/m9.figshare.c.8268142.

THE ROYAL SOCIETY PUBLISHING

Penetrative track morphology and sediment parameters: subsurface layers are robust to changes in substrate properties

Benjamin William Griffin, Tash L. Prescott, Andréas Jannel and Peter Lewis Falkingham

School of Biological and Environmental Sciences, Liverpool John Moores University, Liverpool, UK

BWG, 0000-0001-9454-6212; TLP, 0009-0003-0836-8395; AJ, 0000-0002-6625-5693; PLF, 0000-0003-1856-8377

Track morphology is controlled by the anatomy and motion of the foot, as well as by the consistency of the sediment. Penetrative tracks preserve information regarding the motion of the foot due to increased foot–sediment interaction. The track morphology in subsurface layers of a penetrative track is important for recovering these preserved motions. Using discrete element method simulations, we examined how subsurface track morphology varies with sediment consistency. Two models were used: a vertically indenting cylinder and a dynamic, simplified theropod-like 'tridactyl foot'. For both cases, we systematically changed friction and cohesion and examined changes to subsurface track morphology. Increasing friction (lower 'flowability') resulted in higher and more extensive displacement rims throughout the track volume. Increased cohesion led to tracks remaining open, preventing infilling from above. Low cohesion led to surface tracks deviating substantially from the morphology of the foot, and in cases of very low cohesion, appearing deceptively like weathered tracks. Tracks exposed along subsurface layers had morphologies more robust to changes in sediment properties than the surface tracks. Thus, changes in sediment behaviour significantly affect surface, but not subsurface, track morphology. Our findings support the reliability of motion reconstructions from penetrative tracks, regardless of sediment conditions at the time of formation.

1. Introduction

Fossil tracks preserve a valuable record of vertebrate behaviour through deep time. However, tracks are not exact replicas of the feet that produced them [1]. Instead, track morphology is dependent upon the anatomy of the track maker, the movements of the limb and the consistency of the substrate [1–6].

Since being formalized by the work of Hitchcock [7–10] and his contemporaries [11–13], vertebrate ichnology has focused primarily on surficial or 2.5-dimensional [14] descriptions of morphology and morphometrics (track length, digit impression, divarication, etc.). Examination of track surfaces allows linear measurements to be made at both the individual track and trackway scales to discriminate between track makers with similar pedal morphology [15] and recover overall locomotion trends [4,16–18]. Recent techniques may also incorporate geometric morphometrics of either fixed landmarks or complete track outlines to capture the entirety of the surface morphology (e.g. [19–22]), the most advanced of which include the development of deep learning algorithms to differentiate between tracks and

impartially determine the affinities of the track maker [23,24]. Advances in the capture of three-dimensional track data [25–29] have improved the objectivity and repeatability of vertebrate ichnology, from ichnotaxonomy to quantitative analysis.

Despite a reasonable and practical focus on surface features, tracks are inherently volumetric structures, extending below the original sediment–air (or water) interface. Previously considered as only 'undertracks' (or synonyms thereof), recent work has made clear the distinction between 'transmitted' and 'penetrative' undertracks [30,31]. Transmitted undertracks are deformed sediment beneath the base of the true track [32–37], and penetrative undertracks are where the foot penetrates through multiple layers of sediment, leaving a 'true track' below the original tracking surface [1,30,31,38–40]. Penetration of the foot requires softer or more fluid substrates, while more competent sediment lends itself to transmission of displacement. Because the distinction is relatively recent, previously described 'undertracks' may in fact be penetrative rather than transmitted (e.g. figs. 3 and 4 in [36]).

Penetrative tracks incorporate more of the motion of the foot and its proximal anatomy (e.g. the hallux or metatarsus) into their morphology than surficial tracks [31,41–43]. In rare cases, separation of laminations within the rock, as has been seen in the Hitchcock collections at the Beneski Museum of Natural History (e.g. [31,44]), reveals the full extent of deformation structures of a penetrative track.

Understanding penetrative track morphology requires analysis of the entire three-dimensional track volume. While this information is not readily accessible for the majority of penetrative fossil tracks without excavation and splitting or sectioning, both the use of extant analogues [38,39] and digital modelling approaches [31,39,44] aid in developing the understanding of the processes involved. This combination of simulation with extant taxa validation exemplifies the current state of experimental vertebrate ichnology [45].

Among modelling approaches, discrete element modelling (DEM) stands out for its ability to simulate the interactions between individual particles, or groups of particles within a sediment. DEM allows the creation of repeatable sediment properties and virtual laminations exposing subsurface displacements at varying depths, providing insight into penetrative track morphology and formation [39]. Furthermore, the DEM approach to simulation enables testing of hypothetical motions derived from fossil penetrative tracks, allowing the effects of sediment parameters through the entirety of the formation process to be examined [40,44]. Falkingham *et al*. [44] noted in passing that subsurface track morphology is relatively robust to changes in the substrate consistency, while the morphology at the tracking surface is more variable. The authors attributed this difference to the increased freedom of the surface layers to move and therefore respond to changes in the input properties of the model. However, this hypothesis has not yet been objectively tested beyond preliminary qualitative sensitivity examinations, and quantified data are currently lacking to support it. As a result, a key question emerges: can penetrative tracks preserve consistent information about foot motion and sediment interaction on the surface and at depth across different substrate conditions/parameters? In this study, we aimed to quantify how resistant subsurface tracks are to variations in sediment properties. To achieve this, we used DEM simulations and quantified how sediment parameters affected the morphology of surface and subsurface tracks.

2. Methods

In this study, we conducted experiments using two models of different complexities. All simulations were carried out using the open-source DEM software LIGGGHTS-PFM (v. 24.01, https://github.com/ParticulateFlow/LIGGGHTS-PFM), a variant of the LIGGGHTS software [46] developed by Johannes Kepler University, Linz, Austria.

2.1. Model 1—cylinder

This model used a simple horizontal cylinder with a 4 mm diameter (approximately the width of an adult guineafowl toe) as a basic indenter. To observe the subsurface deformation of the middle section of the cylinder with the substrate, the cylinder moved vertically downwards into a virtual container with dimensions 26 × 25 × 6 mm, containing approximately 65 000 medium sand-sized spherical particles (0.2 mm radius; figure 1A). The container represents a thin slice of sediment beneath the descending 'toe'. Random colouring was applied to particles based on starting vertical (Z) position, so that virtual laminations within the sediment could be visualized. Layers are mechanically identical. While real sediment laminations may have mechanical variations, the penetrative tracks previously described [31,40,44] show no indications of such variations affecting the path of the foot, so we assume consistent properties throughout. The indenter was positioned centrally above the virtual container (figure 1A) and was indented at 20 mm s^{-1} for 1 s to a depth of 20 mm. Gravity followed the Z axis. The simulation used a timestep of 0.000001 s. The simple cylinder allowed observation of changes to surface and subsurface track morphology resulting from alteration of substrate parameters without confounding effects of complex motion and anatomy.

The indenter descended into the simulated sediment to a depth of 20 mm before being extracted vertically upwards through the already deformed layers. Simulations were viewed both at the midpoint and the end of the motion, so both a 'clean' view of deformation resulting purely from entry and a view of deformation after removal of the indenter could be recorded. Particles were given time to settle until stable before the indenter motion began, at the end of the indentation prior to extraction and after the entire motion sequence was completed. These simulations were displacement-controlled. Indeed, the prescribed motion is independent of the resistance of the virtual sediment, enabling descent to the same depth in different substrate types.

Particle parameters of the virtual sediment were modified to ascertain the effects on the simulated deformation of subsurface laminations. The parameters that changed were the cohesion energy density ('stickiness', or how much force is required to move particles in contact apart) and friction coefficient (approximating 'roughness', or how much force is required to move

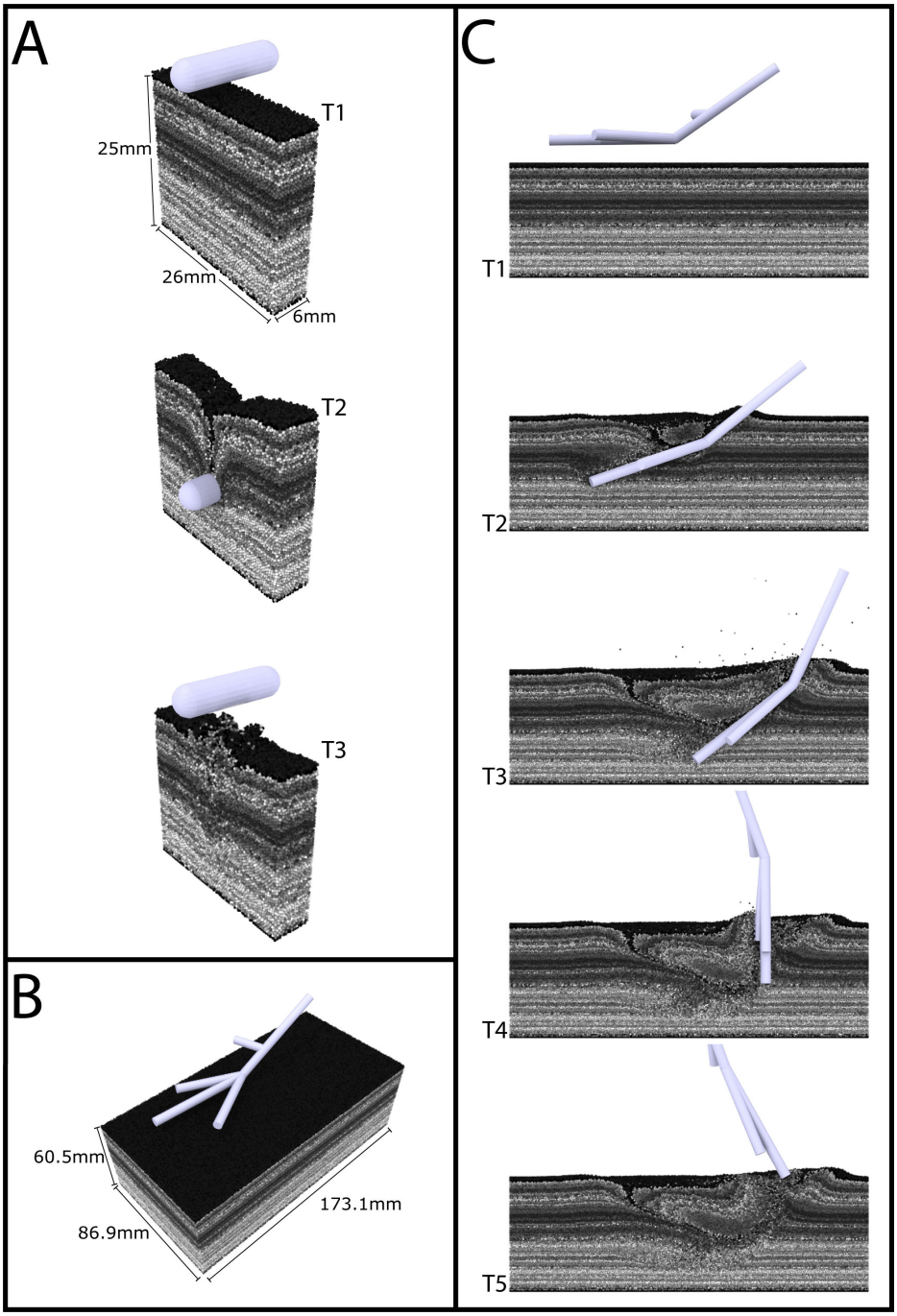

Figure 1. Perspective views of (A) the cylinder (including the motion used) and (B) the animated foot modelling systems with respective sediment volume measurements. (C) The motion of the animated foot model through a lateral cross-section of the animated foot volume (animation frames 0, 90, 180, 270 and 360).

one particle past another in contact). Additional variations, including Young's modulus, the particle contact model and particle size, were tested but not reviewed in detail due to having more minor effects on the resultant trace morphology (see electronic supplementary material). Adjusting friction and cohesion (and to a lesser extent, other variables) enables approximation of bulk behaviour similar to non-spherical particles (e.g. increasing friction has the same effect as making grains less round). Virtual sediment laminations 0.8 mm thick were visualized to examine morphology changes at depth using the following three depths: (i) 0 mm, (ii) 11.6 mm, and (iii) 19.6 mm. These layers are considered representative of the surface track, a midpoint of the penetrative track volume, and just below the deepest point the cylinder sank to. The position of the particles was recorded at the start and end of the simulations to compare the magnitude and direction of displacement between the different layers using a custom R script (electronic supplementary material S1).

2.2. Model 2—animated tridactyl foot

The tridactyl foot model (figure 1B) simulated a tridactyl left foot animated according to reconstructed foot motions of a Jurassic dinosaur. We based our simulation on the virtual foot and associated hypothesis of motion determined by Falkingham *et al.* [44] to explore the effects on a real case of subsurface track morphology. As with the cylinder indenter simulations, the motion is prescribed and unaffected by resistance from interaction with the particles (figure 1C). This motion was derived by matching an

Early Jurassic penetrative track from the Hitchcock collection in the Beneski Museum of Natural History, Amherst (specimens ACM-ICH 31/51, 31/57, 31/58 and 31/59, each number referring to a layer of the track volume) [9,44]. The virtual foot model comprised five cylinders corresponding to the metatarsals and digits 1–4. The foot was functionally tridactyl, with the hallux reconstructed as relatively small and raised on the metatarsals. The foot was moved through a virtual box 86.9 × 173.1 × 60.5 mm containing approximately 2 143 000 particles of 0.4 mm radius (figure 1B).

A series of 12 simulations was run using a subset of the cylinder indenter parameters that showed the range of track morphologies. A subset was used because simulation times for the full foot were orders of magnitude longer than for the simple cylinder case (approx. 4 h versus 35 min using two cores on the Prospero computing cluster at Liverpool John Moores University). Cohesion energy density was varied from 25 000 to 150 000 J m^{-3} at intervals of 25 000 J m^{-3}. These simulations were run with a coefficient of friction of either 0 or 0.8 at Young's Modulus 5.00 × 10^6 Pa, as these values showcased the breadth of morphologies in the cylinder model testing.

Prior to indentation, the particles in each simulation were allowed to settle, and then all simulated particles above a set height were removed, ensuring a consistent Z position of the tracking surface across simulations. Relative to the fossil track volume used to construct the hypothesis of motion, the tracking surface is located 1 mm immediately above the uppermost fossil surface, matching the set-up of Falkingham *et al*. [44]. To compare track morphology at varying depths, virtual layers were exposed by hiding the overlying particles. Depths were chosen corresponding to the exposed laminations of the Amherst specimens, in line with the previous simulations by Falkingham *et al*. [44].

At the end of the simulation, the marks left by each digit tip, the hypex and the exit were recorded as XY positions on each surface. Determining landmarks on non-elite tracks is notoriously difficult due to the smooth transition from track to tracking surface. While attempts can be made to apply objective methods [22,47,48], ultimately, there can still be subjectivity in how those methods are applied [14]. Applying contours, for instance, would not make sense in cases where the surrounding sediment has also collapsed. The relatively coarse nature of our sediment also makes pinpointing features with precision (i.e. to less than one particle diameter) difficult. As such, to locate our landmarks, we applied similar techniques as would be applied to real fossil tracks; colouring the surface according to height (scaled to the max/min of the surface) and then making an informed judgement about where the landmark (e.g. the tip of the toe impression) was.

Variability in track morphology across substrates was calculated in R [49] as the standard deviation (s.d.) for each landmark. The distance from the 'true' passage of the foot was also calculated. The 'true' extent of the anatomical digits was recorded using the same XY coordinate system by locating the animation frame where the indenter first contacted the layer. The true exit was marked at the point where the indenter lost contact with the simulated lamination. As with the cylinder model, individual particle locations were also recorded to examine vertical displacement throughout the track volume.

3. Results

3.1. Model 1—cylinder

Increasing the friction coefficient results in a deeper indentation above the cylinder and an increased upward vertical displacement of the particles around it. The displacement rim peaks occur closer to the path of the cylinder at higher frictional values, resulting from the higher angle of repose. Displacement rims caused by higher friction are more prominent particularly at the surface, but also at deeper levels (figure 2A). Reducing friction to zero results in the uppermost laminations lacking definition and the lowermost level being bowl-like in form, though sharp nested-V shapes are still visible in the laminations between these.

The most notable feature of increased cohesion is that the particles remain open behind the cylinder, held up by the cohesive substrate. There is also an increase in the displacement rim height. Where the trace remains open, the lowest layer no longer directly interacts with the cylinder. Instead, the layer is deformed via the transmission of displacement from the particles above it, which remain together beneath the descending indenter.

Following the extraction of the indenter (figure 2B), the displacement rim is more complex, with the surface trace no longer entirely constructed of the particles that began at the surface level. The displacement rim that is formed is a composite of both the initial insertion displacement and the sediment particles brought to the surface by the indenter. This creates complex morphologies, such as the folding of the surface layer seen in the 75 000 J m^{-3} cohesion model.

The upward extraction creates complex subsurface structures when the sediment is cohesive. Subsurface layers exhibit inverted Vs, drawn upward by the cylinder. The layer deflection is also asymmetrical—a result of the particles above the indenter falling together to one side or the other. The lowest lamination maintains a largely symmetrical shape.

3.2. Model 2—animated tridactyl foot

The animated foot simulations (figure 1B) result in functionally tridactyl elongate tracks that show a high degree of variation in surface morphology associated with changes to cohesion and friction, but low variation at subsurface levels (figures 3 and 4). The trends in cohesion and friction seen in the cylinder simulations remain consistent for the animated foot simulations—increasing friction results in larger displacement rims, and increasing cohesion results in 'open' rather than 'sealed' tracks (figures 3 and 4).

The surface tracks show increases in the height and extent of the displacement rim as both the friction and cohesion of the sediment are increased, though the effect is greater for friction than for cohesion. In the lower friction simulations, the angle of

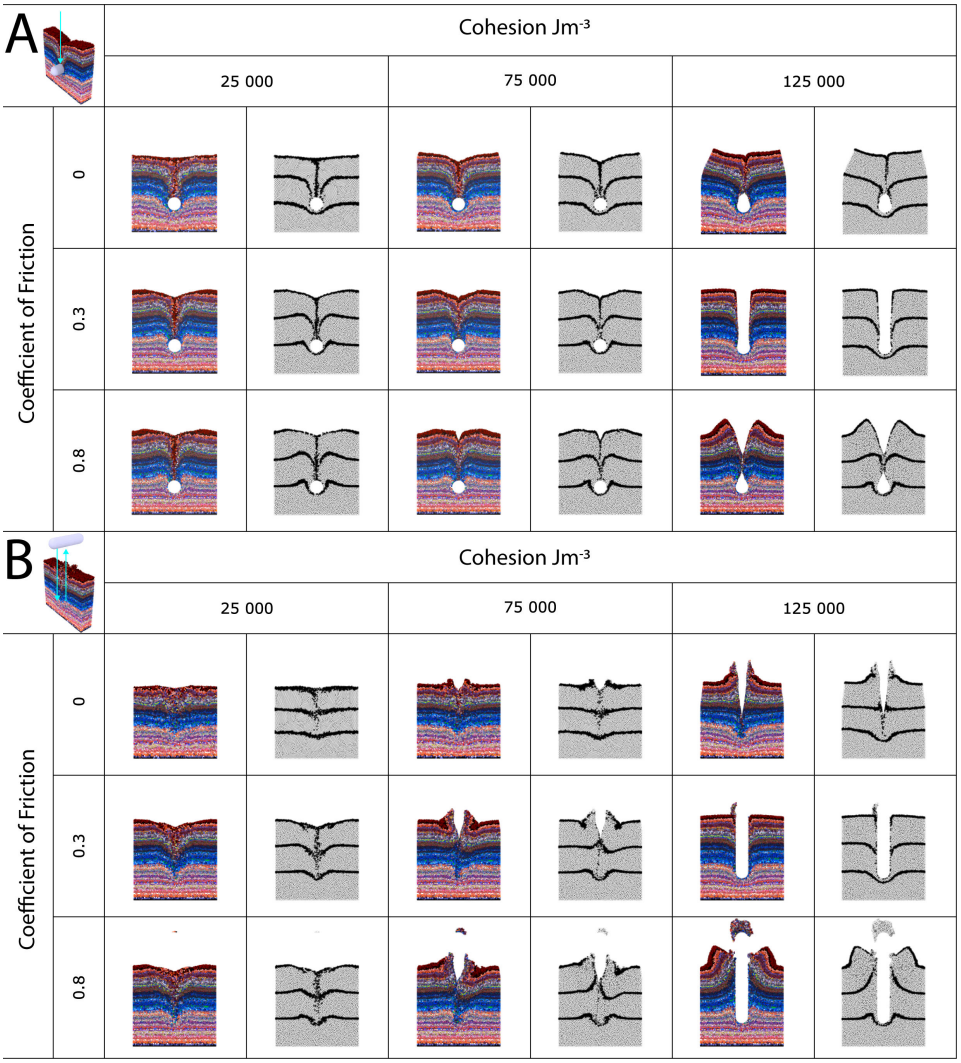

Figure 2. A subset of the cylinder model simulations showing sediment particle deformations at two time steps. Paired images compare exposed layers used for examination (right) with the entire sediment volume (left). (A) The midpoint of the cylinder motion. This provides an indication of the layer deformations caused purely by indenter entry. (B) The end of the cylinder motion. This demonstrates the more complex deformations following the exit of the indenter for the same subset of cylinder simulations. For the full set of cylinder simulations, see electronic supplementary material.

repose is reduced, meaning particles flow in to fill the trace, creating a shallower surface track with lower displacement rims. The largest positive vertical displacement in all cases occurs around the exit trace, even in the most fluid of substrates.

In the subsurface layers, changes resulting from increases in friction are more subtle than those resulting from cohesion, the exception being the exit mark. Primarily, increased friction causes higher displacement rims and deeper traces. The exit trace shows a substantial positive vertical displacement with increased friction in all but the lowest depth (44 mm; figure 4). Perhaps counterintuitively, increased cohesion results in a narrowing of the impression in the subsurface layers. Particles from higher up do not fall into the trace, and the walls are allowed to collapse inwards. This aligns with the shift of the displacement rim towards the centre seen in the cylinder model. Despite the narrowing of the toe and metatarsal impressions and positive vertical displacement around the exit trace, the overall morphology on the subsurface layers is far more consistent than the morphology of the surface layer.

We also examined the displacement throughout the step cycle (electronic supplementary material S2). During the first half of the stance phases, the largest vertical displacement is primarily negative, with the highest total vertical displacement consistently found in the surface level particles. The average displacement for the entire sediment volume, however, is slightly positive as the sediment is displaced to account for the volume of the indenter and the formation of the initial displacement rim. In the second half of the stance phase, as the foot is extracted from the sediment, particles from deeper zones are pulled up, and the exit displacement rim is formed. These deeper particles moving upwards experience the greatest total displacement within the sediment volume, resulting in a substantial increase in the magnitude of positive vertical displacement. The increased range of displacement is especially evident in the 17–29 mm depth layers, which experience moderate negative displacement during the first half of the stance phase, before large displacements upwards, essentially being 'hit twice' by the foot passing through the particles on both entry and exit. Though the surface is also 'hit twice' by the foot motion, the lack of constraining sediment above allows particles to move laterally and experience less total upward motion.

Landmark data (figures 5 and 6) revealed a greater variability in coordinate positions on the surface than in the subsurface layers. Precision, defined here as reduced s.d. between the landmarks, varied markedly at the surface layer and improved with depth. The surface landmarks ranged from an average s.d. of 5.27 mm for digit III to 1.39 mm for the hypex (mean 2.69 mm;

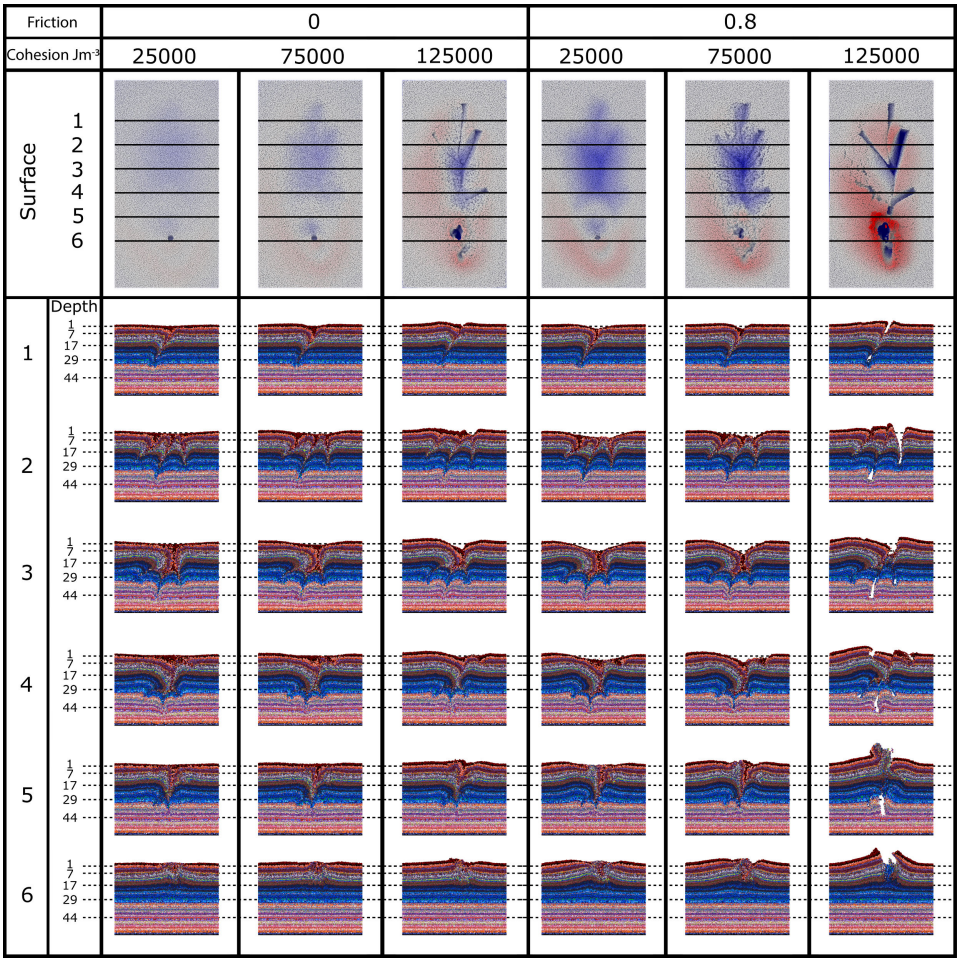

Figure 3. Cross-sections of the animated foot model for a representative subset of sediment consistencies. The top-down surface images show the cross-section locations and demonstrate the variability of the trace morphology. The cross-sections demonstrate the consistency of the nested-V morphology in the traces across sediment consistencies. Depth markings highlight the position of the subsurface layers displayed in figure 4. An expanded version of this figure is included in the electronic supplementary material.

figure 6A). Even 1 mm of depth improved the average precision to 2.10 mm. At depths below 7 mm, the largest deviation for any landmark was 2.10 mm (exit at 17 mm depth) with averages of 1.21, 1.31, 1.34 and 1.29, respectively. Landmark accuracy, herein defined as reduced s.d. from the 'true' location of each landmark, showed an increase with depth (figure 6B). The average landmark accuracy per layer improved from 4.37 mm at the surface to a low of 2.41 mm at 7 mm depth. The least accurate landmark was digit III, which had an average s.d. of 7.35 mm from the 'true' location at the surface; however, this rapidly decreased with depth. Of the landmarks, only the exit showed a consistent reduction in accuracy as depth increased. In general, the position of the foot's hypex tended to be the hardest point to confidently reconstruct from track images, due in part to the posterior sliding and undercutting by the indenter, causing sediment to slump. Despite this difficulty, the approach to placing this landmark resulted in high precision, roughly equivalent to that of digit II. The difficulty in placement was instead reflected in the lower accuracy of the landmark on each of the layers where it occurs. Digit I tended to have the lowest variance both in terms of precision and accuracy across the examined layers. When each sediment consistency is reviewed individually, there is a clear increase in landmark accuracy with sediment cohesion (figure 6C). While the low cohesion simulations show a drastic increase in accuracy with depth, at cohesion values exceeding 100 000 J m^{-3}, the accuracy of the surface landmarks improves sufficiently to equal and, in some cases, exceed the accuracy at depth. This matches with the qualitative reduction in landmark definition seen in the most flowable substrate models (figure 7A)

4. Discussion

4.1. Effects of cohesion and friction on track volume morphology

Surface tracks are more sensitive to changes in sediment properties than subsurface tracks. Across both our models, we observe substantially greater qualitative and quantitative variation in tracks at the tracking surface compared with subsurface layers (figures 3–6). Virtually exposed subsurface laminations remain highly consistent in all but the most cohesive and frictional substrate, yet surface features differ considerably. At the surface, more flowable sediment (i.e. low cohesion and low friction) can infill the entry behind (above) the indenter. Once the particles infilled the space made by the indenter, the particles, and thus the sediment, become constrained. As a result, irrespective of sediment properties, particles are limited in flow around the indenter, producing similar subsurface tracks for a given motion and anatomy.

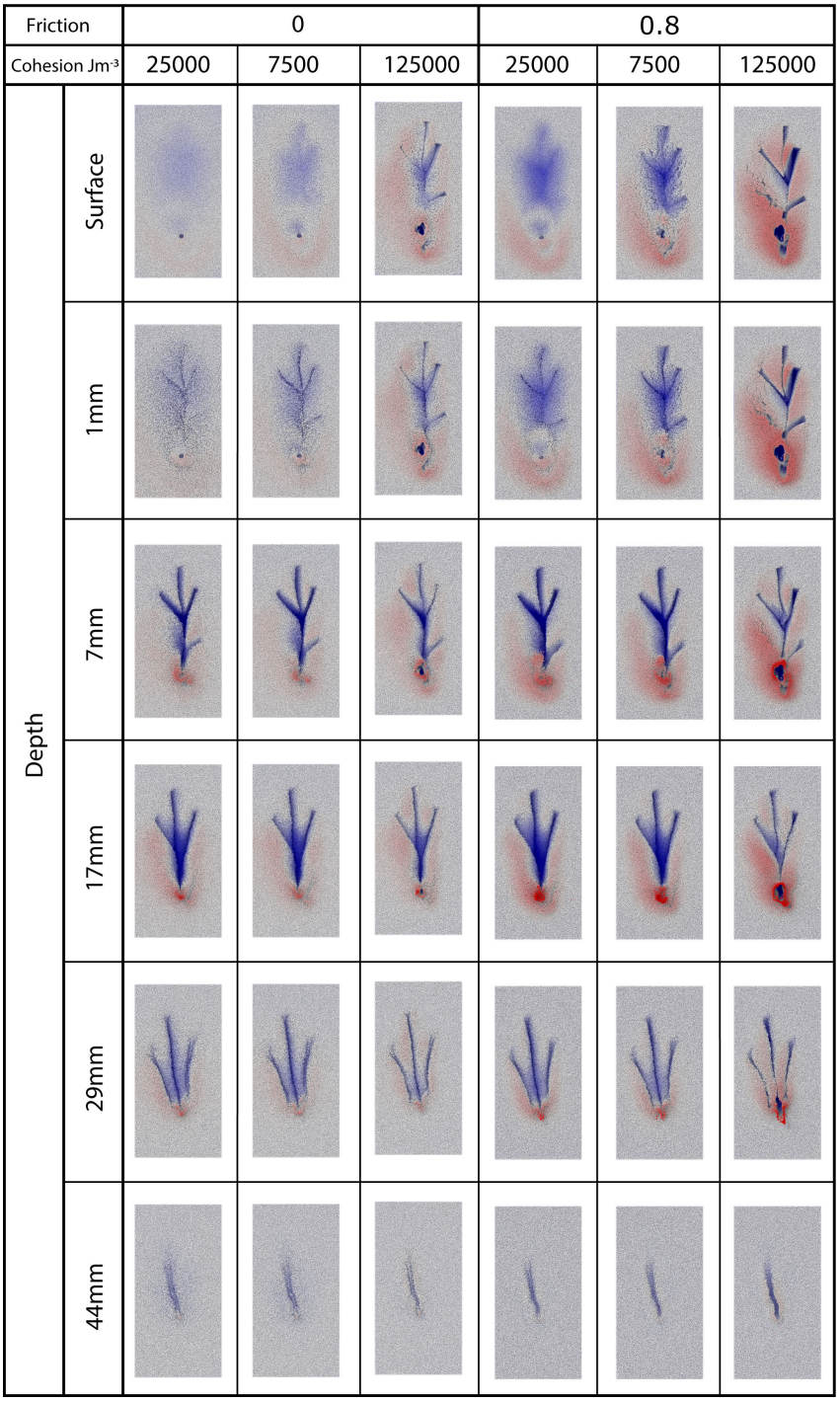

Figure 4. Top-down views of the surface and exposed subsurfaces in the animated foot model. The exposed depths are equivalent to those of Falkingham *et al.* [44] and correspond to the exposed surfaces of the Amherst track volume. The surfaces have been coloured with an exaggerated colour scale (red→blue = 10 mm) to better highlight the deformation trends with changes in cohesion and friction. For an expanded version of this figure, check the electronic supplementary material.

4.1.1. Digit tips

The digit tip impressions are highly variable at the tracking surface, especially at lower cohesion (figures 5 and 6). Digit III, the middle digit, is particularly prone to high surface deviation (figure 6A,B). As digit III is the first point of contact, and because the motion of the foot includes a posterior slide, the anterior-most point of the trace is shallow. In the lower friction and cohesion simulations, the anterior-most point of the trace collapses completely, leaving minimal vertical displacement. At depth, infill maintains the position of this landmark. This has implications for the estimation of foot length and comparative length of the toes in low-cohesion and low-friction tracks, causing both to be underestimated on the surface layer. Reduction in foot length has follow-on effects to estimations of hip height and subsequent estimations of speed [50,51], while the variation in toe length makes the reconstruction of a hypothesis of motion less straightforward, as it varies between layers. This shortening is accounted for by the assumptions of the toe length being the minimum required to make the fossilized trace when the digital foot and motion were originally modelled [44], but is unlikely to be considered when examining tracks or estimating the proportions of the track maker in the field.

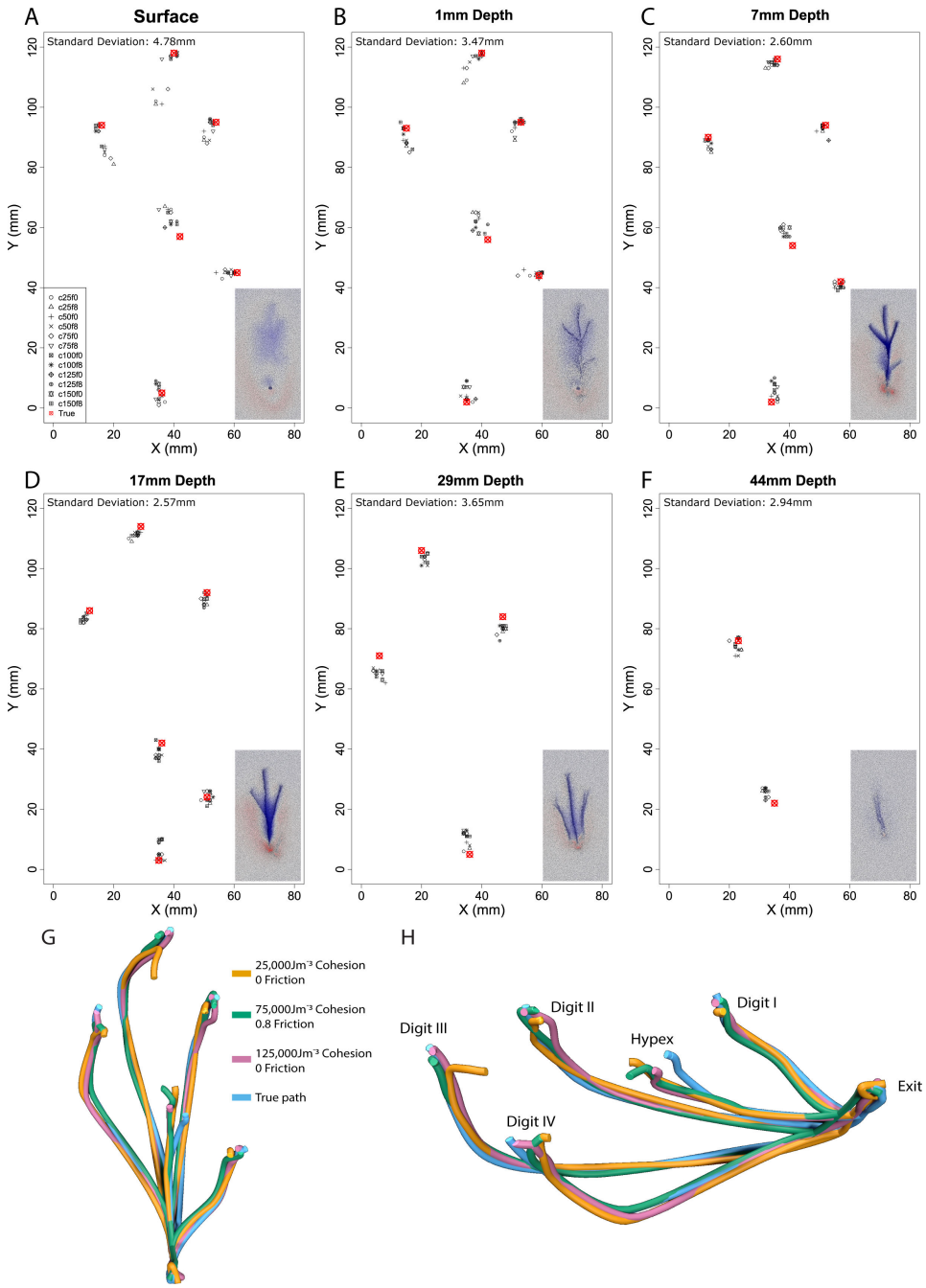

Figure 5. (A–F) XY plots presenting the landmark locations for each sediment consistency in each examined layer. Inset image of the track of the 75 000 cohesion, 0 friction model provided to aid in orientation and context. Red points indicate the 'true' landmark where the digit first contacted the surface or last contacted the surface in the case of the exit landmark. s.d. values show average deviation from the 'true' landmark (landmark accuracy) for the entire layer. (G,H) The three-dimensional variation as example reconstructions of the digit paths through sediment in top-down (G) and perspective views (H).

The impression of digit IV is more variable at the surface than digit II, despite being equal in length and contacting the surface simultaneously. The motion of the foot has a lateral component, rotating towards digit IV during indentation. This causes slumping of the sediment that is undercut, shifting the mark left by digit IV. While this is unlikely to cause any ichnotaxonomic confusion in a trackway where the lateral motion would either be mirrored in the next track or was a single irregularity, for isolated tracks, this may result in an incorrect estimation of the foot morphology.

Perhaps most interesting is the consistently low variation in the positioning of the hallux trace. In the low-friction and low-cohesion simulations, the hallux trace is so shallow that it barely leaves any impression, yet due to its isolated position on the metatarsals, the position can still be marked with reasonable accuracy. This would not be the case in a posteriorly directed hallux, as the trace would be overprinted by the metatarsals in deep tracks and the exit trace in broad looping motions such as the motion used in this study.

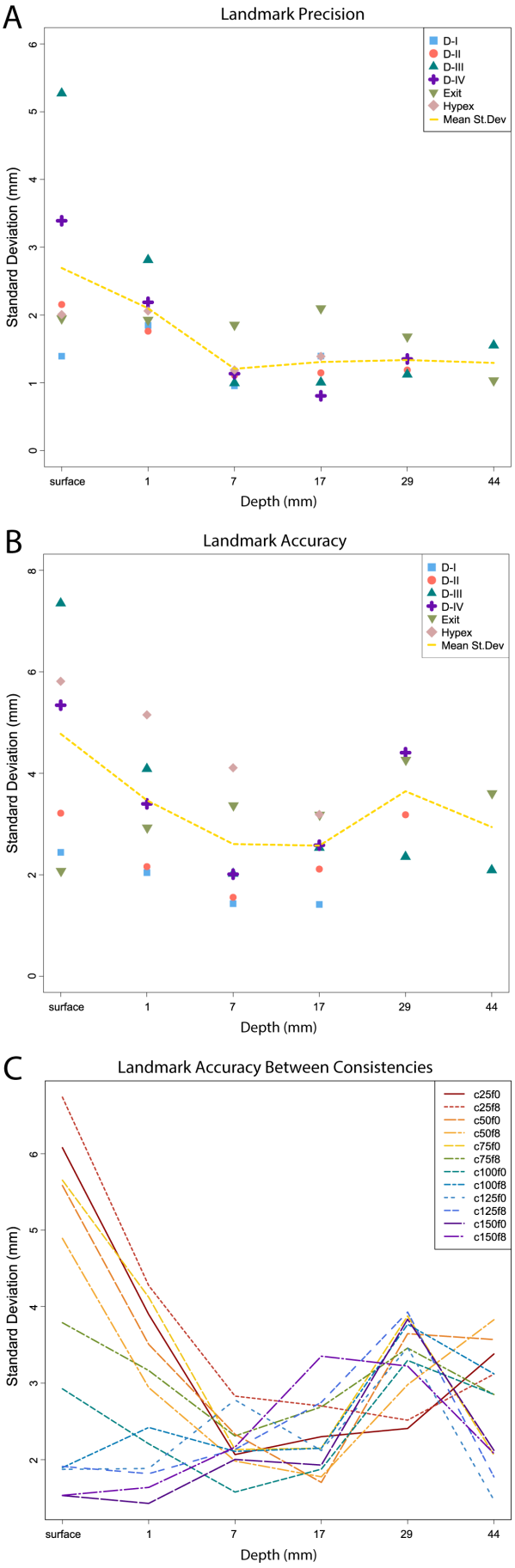

Figure 6. (A) Scatter plot of landmark precision in the animated foot model. Landmark precision is defined as reduction in the average divergence in landmark position across consistencies. The plot shows an average improvement with increased depth before plateauing below 7 mm. (B) Scatter plot of landmark accuracy, defined as a reduction in deviation from the 'true' landmark, shows a similar trend to landmark precision. (C) Line graph illustrating the landmark accuracy between the sediment consistencies tested. There is a clear increase in landmark accuracy with increased sediment cohesion.

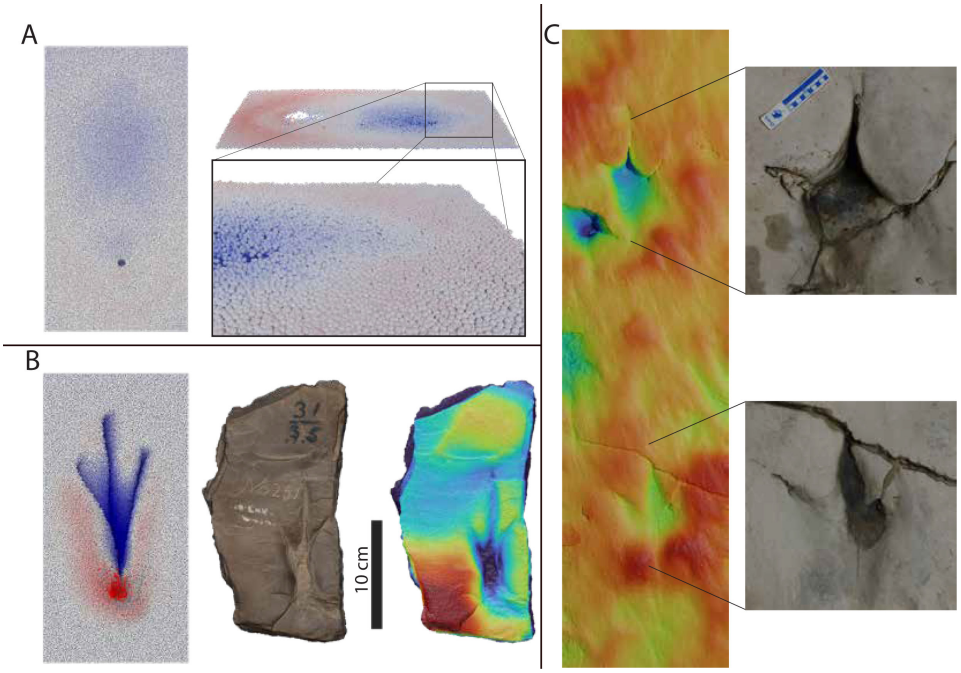

Figure 7. (A) Surface track made in highly flowable substrate (cohesion 25 000, friction 0), presented in perspective views with exaggerated colour scale (red→blue = 10 mm) to indicate the difficulty in defining landmarks on the surface. (B) Simulation and comparative fossil track from the Hitchcock collection (ACH-ICH 31-35) showing the posterior depression indicative of backward foot movement. (C) Two theropod tracks from a trackway at Glen Rose, Texas; tracks on this surface appear to have been made in deep, soft sediment, with partially sealed digit traces (top); yet the prior track (bottom) appears relatively shallow and the base of the impression appears continuous with the tracking surface, potentially indicating this was a deeper track that has completely sealed, as in some of the surface tracks in our simulations.

4.1.2. Exit

Variability in exit location increased with depth because the feature itself becomes less obvious. The variation at depth is most commonly an underestimation of the posterior extent of the exit. This is an interesting mirror of the tracking of digit III, which becomes more accurate with depth.

4.1.3. Hypex

With the exception of digit III at the surface, the hypex has the largest variability of the measured points (figure 6). This is because the hypex is generally difficult to accurately measure since the convergence point of the three digits is not clear, even in the higher cohesion and friction simulations. The uneven filling of the trace due to slumping of the particles from undercutting further obscures its location. Variability in hypex coordinates is therefore less an indication of the hypex trace moving relative to the foot and more a representation of the vagueness of the feature itself.

4.1.4. Comparison between simulations and fossil tracks

With increasing cohesion, particles can support each other laterally and cannot easily move into open spaces. Near the surface, this increase causes improved track fidelity, while in the lower layers, the effects are less obvious. At lower cohesion, particles are able to fall back into the void left behind the indenter (either the cylinder or the foot). This results in a fully sealed track. At low cohesion, or moderate cohesion with low friction, the surface trace becomes indistinct, resembling either a weathered track or an indistinct track made by a much thicker-toed foot. Despite the striking differences at the surface, subsurface tracks remain highly similar to each other both in terms of cross-section (figure 3) and subsurface topography (figure 4).

At the highest cohesion, the tracks remain open after the indenter or foot has been removed. In fossil tracks, this opening will be infilled by sedimentation. After exposure, the infill may be eroded preferentially if the sediment is softer than the rock in which the track is preserved. Conversely, the infill may remain as a positive cast if stronger than the surrounding rock. It may also break partially within the track, potentially creating a false bottom [31]. Such infill is the proposed preservation process for natural moulds such as the three-dimensional convex hyporelief tracks from the Costalomo tracksite in Spain [52] and the toe cavities reported from the Paluxy Riverbed in the USA [53]. The high cohesion tracks also record high consistency in subsurface morphology, indicating that these natural moulds are likely to be accurate pending changes during the process of preservation after the track has fully formed.

While the surface layer tends to produce broad, poorly defined tracks in all but the most cohesive, low-friction sediments, even a 1 mm depth improves the fidelity of the track, more closely matching the narrow-toed morphology associated with penetrative tracks. Similarly, the cross-section showcases the characteristic penetrative nested-V-shaped structure in all but the topmost surface of the track volume. Although no virtual layer perfectly captured the morphology of the indenter, the

track volume consistently preserved a traceable sequence of the indenter motion. The simulations also reliably produced a pronounced posterior depression (figure 7B), which we interpret as a pronounced backwards movement of the foot, similar to that observed in other fossil tracks such as ACH-ICH 31-35 from the Hitchcock collection in Amherst.

For the avoidance of doubt, we are not suggesting that all tracks will be the same regardless of substrate consistency. The interaction between track maker and substrate is complex and interrelated: softer substrates both necessitate and cause different movements, some intentional by the track maker, others passive in how the foot responds to the deforming substrate [40,54]. However, our simulations demonstrate that a given movement of the foot will be reliably recorded in subsurface penetrated layers, with details retained even in highly flowable substrates by the surrounding confining substrate.

4.2. Implications for interpreting fossil tracks

The difference in variability between the surface and subsurface tracks has implications for the interpretation of penetrative track fossils in the field. Of the three components that control track morphology (anatomy, motion and sediment), sediment consistency is particularly difficult to determine for fossil tracks. Consistency (cohesion and friction) is highly dependent upon water content, a factor not preserved and difficult to constrain in fossil tracks [4]. While some studies have attempted to calculate water content at the time of track formation [55], the results had a wide margin of error. Even small changes in water content can substantially affect sediment behaviour, making the estimates based off these calculations tenuous at best for fossil tracks. If the track morphology varied significantly as water content increased, we would not be able to rely on track-based landmarks to reconstruct foot motion paths.

Fortunately, despite the high degree of variability in surface track morphology with substrate consistency, subsurface track morphology appears to be highly resistant to changes in sediment parameters. This outcome reassuringly provides a level of confidence when constructing hypotheses of motion [17,42,44]. Robust subsurface track morphology means that even if the sediment conditions at the time of track formation are not well constrained, a penetrative track can still provide accurate kinematic information.

The sediment-dependent nature of the tracks at the surface is important, given that some authors (e.g. [56]) argue ichnotaxonomic assignment should require 'elite' surface tracks. It is already widely acknowledged that track morphology is dependent on sediment conditions at the time of formation [30,34,36,37] and that such sediment conditions are difficult to reconstruct. Our simulated tracks over a range of friction and cohesion values (while maintaining anatomy and kinematics) aptly demonstrate how much tracks can vary purely through sediment properties (figure 4).

Our less well-defined surface tracks observed in the least cohesive, and especially least frictional, substrates (i.e. those most able to flow) bear a striking resemblance to tracks that might otherwise be considered poorly preserved true tracks. Yet by definition, *sensu* Gatesy & Falkingham [1], Falkingham & Gatesy [57] and see Lallensack *et al.* [30], our simulations are perfectly preserved, and indeed the traces retain anatomical and kinematic features from shallow depths below the tracking surface. Notably, the surface impressions in these simulations appear to have far thicker toes, a key factor in assigning potential track makers (e.g. between birds and dinosaurs). What makes this particularly concerning for ichnological identification in the field is that the flowable sediment will produce a continuous sediment surface across the track, making a penetrative origin particularly difficult to identify (figure 7C). This surface may resemble a sediment drape laid over the penetrative track, but in fact, it comprises the original tracking surface.

Our research highlights that a wealth of information about the track maker may be locked within the track volume. Admittedly, the additional information provided by penetrative tracks is not readily available without access to subsurface layers. In some instances, track volumes are naturally (or deliberately) split along laminations [7,31]. Alternatively, advanced imaging techniques (e.g. computed tomography (μCT)) may be able to visualize internal structures, though the lack of density contrast between lithified layers makes this difficult. Our model is, of course, highly abstracted and simplified compared with the messy reality of sedimentology and fossilization, yet it provides a fundamental framework on which to build.

5. Conclusions

In order to quantify how resistant subsurface tracks are to changes in sediment consistency, our study simulated penetrative track formation across a range of substrate friction and cohesion values using DEM simulations. Our results show that changes to simulated substrate properties resulted in drastically varying surface track morphology, while the morphology of the subsurface penetrative undertracks was surprisingly robust, as quantified by analogous landmarks. In rare cases where a track volume is exposed at multiple depths or when splitting along laminations is possible, the subsurface morphology preserves reliable information about foot kinematics, irrespective of sediment properties at the time of track formation.

Ethics. This work did not require ethical approval from a human subject or animal welfare committee.

Data accessibility. All scripts used for simulation have been included in the supplementary material [58].

Declaration of AI use. AI has been used solely to enhance the clarity of the code used for processing data (adding annotations, streamlining of loops for more efficient coding). All AI code was independently checked and verified as functional prior to final implementation. AI was not used in any of the writing or data interpretation in this manuscript.

Authors' contributions. B.W.G.: conceptualization, data curation, formal analysis, investigation, methodology, visualization, writing—original draft; T.L.P.: investigation, visualization, writing—review and editing; A.J.: investigation, visualization, writing—review and editing; P.L.F.:

conceptualization, data curation, funding acquisition, investigation, methodology, project administration, resources, software, supervision, visualization, writing—review and editing.

All authors gave final approval for publication and agreed to be held accountable for the work performed therein.

Conflict of interest declaration. We declare we have no competing interests.

Funding. This work was funded by UKRI Frontier Research Grant TRACKEVOL (selected by the ERC for a consolidator award) awarded to P.L.F.

Acknowledgements. We would like to thank Paige de Polo and Oliver Demuth for helpful discussions on this topic. We would also like to thank the two anonymous reviewers for their helpful insights, which have greatly improved the quality of this paper.

References

1. Gatesy SM, Falkingham PL. 2017 Neither bones nor feet: track morphological variation and 'preservation quality'. *J. Vertebr. Paleontol.* **37**, e1314298. (doi:10.1080/02724634.2017.1314298)
2. Padian K, Olsen PE. 1984 The fossil trackway *Pteraichnus*: not pterosaurian, but crocodilian. *J. Paleontol.* **58**, 178–184.
3. Minter NJ, Braddy SJ, Davis RB. 2007 Between a rock and a hard place: arthropod trackways and ichnotaxonomy. *Lethaia* **40**, 365–375. (doi:10.1111/j.1502-3931.2007.00035.x)
4. Falkingham PL. 2014 Interpreting ecology and behaviour from the vertebrate fossil track record. *J. Zool.* **292**, 222–228. (doi:10.1111/jzo.12110)
5. Razzolini NL, Vila B, Castanera D, Falkingham PL, Barco JL, Canudo JI, Manning PL, Galobart A. 2014 Intra-trackway morphological variations due to substrate consistency: the El Frontal dinosaur tracksite (Lower Cretaceous, Spain). *PLoS One* **9**, e93708. (doi:10.1371/journal.pone.0093708)
6. Abrahams M, Bordy EM, Knoll F, Farlow JO. 2022 Theropod tridactyl tracks across the Triassic–Jurassic boundary in Southern Africa: implications for pedal morphology evolution. *Front. Ecol. Evol* **10**, 925313. (doi:10.3389/fevo.2022.925313)
7. Hitchcock E. 1836 Description of the foot marks of birds, (*Ornithichnites*) on the new red sandstone in Massachusetts. *Am. J. Sci.* **29**, 307–340.
8. Hitchcock E. 1844 Report on ichnolithology, or fossil footmarks, with a description of several new species, and the coprolites of birds, from the valley of Connecticut River, and of a supposed footmark from the valley of Hudson River. *Am. J. Sci* **47**, 292–325.
9. Hitchcock E. 1858 *Ichnology of New England: a report on the sandstone of the Connecticut Valley especially its fossil footmarks, made to the government of the commonwealth of Massachusetts*, p. 220. Boston, MA, USA: William White.
10. Hitchcock E. 1865 *Supplement to the ichnology of New England: a report to the government of Massachusetts*, p. 96. Boston, MA, USA: Wright & Potter.
11. Duncan H. 1828 XI. An account of the tracks and footmarks of animals found impressed on sandstone in the quarry of Corncockle Muir, in Dumfriesshire. *Trans. R. Soc. Edinb. Earth Sci.* **11**, 194–209. (doi:10.1017/S0080456800021906)
12. Kaup JJ. 1835 Über Thierfährten bei Hildburghausen. *Neues Jahrb. Für Mineral. Geol. Und Paläontol* **1835**, 327–328.
13. Pemberton SG, Gingras M. 2003 The Reverend Henry Duncan (1774–1846) and the discovery of the first fossil footprints. *Ichnos* **10**, 69–75. (doi:10.1080/10420940390255574)
14. Falkingham PL. 2016 Applying objective methods to subjective track outlines. In *Dinosaur tracks: the next steps* (eds PL Falkingham, D Marty, A Richter), pp. 72–81. Bloomington, IN, USA: Indiana University Press.
15. Falk AR, Martin LD, Hasiotis ST. 2011 A morphologic criterion to distinguish bird tracks. *J. Ornithol*. **152**, 701–716. (doi:10.1007/s10336-011-0645-x)
16. Ishigaki S, Lockley MG. 2010 Didactyl, tridactyl and tetradactyl theropod trackways from the Lower Jurassic of Morocco: evidence of limping, labouring and other irregular gaits. *Hist. Biol.* **22**, 100–108. (doi:10.1080/08912961003789867)
17. Avanzini M, Piñuela L, García-Ramos JC. 2012 Late Jurassic footprints reveal walking kinematics of theropod dinosaurs. *Lethaia* **45**, 238–252. (doi:10.1111/j.1502-3931.2011.00276.x)
18. Lallensack JN, Falkingham PL. 2022 A new method to calculate limb phase from trackways reveals gaits of sauropod dinosaurs. *Curr. Biol*. **32**, 1635–1640.(doi:10.1016/j.cub.2022.02.012)
19. Castanera D, Colmenar J, Sauqué V, Canudo JI. 2015 Geometric morphometric analysis applied to theropod tracks from the Lower Cretaceous (Berriasian) of Spain. *Palaeontology* **58**, 183–200. (doi:10.1111/pala.12132)
20. Lallensack JN, van Heteren AH, Wings O. 2016 Geometric morphometric analysis of intratrackway variability: a case study on theropod and ornithopod dinosaur trackways from Münchehagen (Lower Cretaceous, Germany). *PeerJ* **4**, e2059. (doi:10.7717/peerj.2059)
21. Costa-Pérez M, Moratalla JJ, Marugán-Lobón J. 2019 Studying bipedal dinosaur trackways using geometric morphometrics. *Palaeontol. Electron*. **22**, 1–13. (doi:10.26879/980)
22. Lallensack JN. 2019 Automatic generation of objective footprint outlines. *PeerJ* **7**, e7203. (doi:10.7717/peerj.7203)
23. Lallensack JN, Romilio A, Falkingham PL. 2022 A machine learning approach for the discrimination of theropod and ornithischian dinosaur tracks. *J. R. Soc. Interface* **19**, 20220588. (doi:10.1098/rsif.2022.0588)
24. Jones M, Lallensack JN, Jarman I, Falkingham P, Siekmann I. 2024 Classification of dinosaur footprints using machine learning. *J. Vertebr. Paleontol.* **44**, e2493157. (doi:10.1080/02724634.2025.2493157)
25. Bates KT, Manning PL, Vila B, Hodgetts D. 2008 Three-dimensional modelling and analysis of dinosaur trackways. *Palaeontology* **51**, 999–1010. (doi:10.1111/j.1475-4983.2008.00789.x)
26. Falkingham P. 2012 Acquisition of high resolution three-dimensional models using free, open-source, photogrammetric software. *Palaeontol. Electron.* **15**, 1–15. (doi:10.26879/264)
27. Matthews NA, Noble T, Breithaupt BH. 2016 Close-range photogrammetry for 3-D ichnology: the basics of photogrammetric ichnology. In *Dinosaur tracks: the next steps* (eds PL Falkingham, D Marty, A Richter), pp. 28–55. Bloomington, IN, USA: Indiana University Press.
28. Davies TG *et al*. 2017 Open data and digital morphology. *Proc. R. Soc. B* **284**, 20170194. (doi:10.1098/rspb.2017.0194)
29. Falkingham PL *et al*. 2018 A standard protocol for documenting modern and fossil ichnological data. *Palaeontology* **61**, 469–480. (doi:10.1111/pala.12373)
30. Lallensack JN, Leonardi G, Falkingham PL. 2025 Glossary of fossil tetrapod tracks. *Palaeontol. Electron.* **27**, 1–105. (doi:10.26879/1389)
31. Gatesy SM, Falkingham PL. 2020 Hitchcock's Leptodactyli, penetrative tracks, and dinosaur footprint diversity. *J. Vertebr. Paleontol*. **40**, e1781142. (doi:10.1080/02724634.2020.1781142)
32. Allen JRL. 1989 Short Paper: Fossil vertebrate tracks and indenter mechanics. *J. Geol. Soc. Lond.* **146**, 600–602. (doi:10.1144/gsjgs.146.4.0600)
33. Allen JRL. 1997 Subfossil mammalian tracks (Flandrian) in the Severn Estuary, S. W. Britain: mechanics of formation, preservation and distribution. *Phil. Trans. R. Soc. B* **352**, 481–518. (doi:10.1098/rstb.1997.0035)

34. Manning PL. 2004 A new approach to the analysis and interpretation of tracks: examples from the dinosauria. *Geol. Soc. Lond. Spec. Publ*. **228**, 93–123. (doi:10.1144/gsl.sp.2004.228.01.06)
35. Milàn J, Bromley RG. 2006 True tracks, undertracks and eroded tracks, experimental work with tetrapod tracks in laboratory and field. *Palaeogeogr. Palaeoclimatol. Palaeoecol.* **231**, 253–264. (doi:10.1016/j.palaeo.2004.12.022)
36. Milàn J, Bromley RG. 2007 The impact of sediment consistency on track and undertrack morphology: experiments with emu tracks in layered cement. *Ichnos* **15**, 19–27. (doi:10.1080/10420940600864712)
37. Jackson SJ, Whyte MA, Romano M. 2010 Range of experimental dinosaur (*Hypsilophodon foxii*) footprints due to variation in sand consistency: how wet was the track? *Ichnos* **17**, 197–214. (doi:10.1080/10420940.2010.510026)
38. Ellis R, Gatesy S. 2013 A biplanar X-ray method for three-dimensional analysis of track formation. *Palaeontol. Electron.* **16**, 1–16. (doi:10.26879/324)
39. Falkingham PL, Gatesy SM. 2014 The birth of a dinosaur footprint: subsurface 3D motion reconstruction and discrete element simulation reveal track ontogeny. *Proc. Natl Acad. Sci. USA* **111**, 18279–18284. (doi:10.1073/pnas.1416252111)
40. Turner ML, Falkingham PL, Gatesy SM. 2020 It's in the loop: shared sub-surface foot kinematics in birds and other dinosaurs shed light on a new dimension of fossil track diversity. *Biol. Lett*. **16**, 20200309. (doi:10.1098/rsbl.2020.0309)
41. Gatesy S. 2003 Direct and indirect track features: what sediment did a dinosaur touch? *Ichnos* **10**, 91–98. (doi:10.1080/10420940390255484)
42. Gatesy SM, Middleton KM, Jenkins Jr FA, Shubin NH. 1999 Three-dimensional preservation of foot movements in Triassic theropod dinosaurs. *Nature New Biol*. **399**, 141–144. (doi:10.1038/20167)
43. Lallensack JN, Farlow JO, Falkingham PL. 2022 A new solution to an old riddle: elongate dinosaur tracks explained as deep penetration of the foot, not plantigrade locomotion. *Palaeontology* (ed. L Marchetti), **65**, e12584. (doi:10.1111/pala.12584)
44. Falkingham PL, Turner ML, Gatesy SM. 2020 Constructing and testing hypotheses of dinosaur foot motions from fossil tracks using digitization and simulation. *Palaeontology* (ed. L Cavin), **63**, 865–880. (doi:10.1111/pala.12502)
45. Milàn J, Falkingham PL. 2016 Experimental and comparative ichnology. In *Dinosaur tracks: the next steps* (eds PL Falkingham, D Marty, A Richter), pp. 15–27. Bloomington, IN, USA: Indiana University Press.
46. Kloss C, Goniva C, Hager A, Amberger S, Pirker S. 2012 Models, algorithms and validation for opensource DEM and CFD-DEM. *Prog. Comput. Fluid Dyn. Int. J*. **12**, 140–152. (doi:10.1504/pcfd.2012.047457)
47. Belvedere M, Ernst S, Marty D. 2016 The precision of outline drawings: a comparison based on dinosaur tracks. In *4th Int. Congress on Ichnology*, Idanha-a-Nova, 6–9 May 2016, pp. 224–225.
48. Belvedere M, Bennett MR, Marty D, Budka M, Reynolds SC, Bakirov R. 2018 Stat-tracks and mediotypes: powerful tools for modern ichnology based on 3D models. *PeerJ* **6**, e4247. (doi:10.7717/peerj.4247)
49. R Core Team. 2025 R: A language and environment for statistical computing. Vienna, Austria: R foundation for statistical computing. See https://www.R-project.org/.
50. Alexander RM. 1976 Estimates of speeds of dinosaurs. *Nature* **261**, 129–130.
51. Prescott TL, Griffin BW, Demuth OE, Gatesy SM, Lallensack JN, Falkingham PL. 2025 Speed from fossil trackways: calculations not validated by extant birds on compliant substrates. *Biol. Lett.* **21**, 20250191. (doi:10.1098/rsbl.2025.0191)
52. Huerta P, Fernández-Baldor FT, Farlow JO, Montero D. 2012 Exceptional preservation processes of 3D dinosaur footprint casts in Costalomo (Lower Cretaceous, Cameros Basin, Spain). *Terra Nova* **24**, 136–141. (doi:10.1111/j.1365-3121.2011.01047.x)
53. Farlow JO, O'brien M, Kuban GJ, Dattilo BF, Bates KT, Falkingham PL. 2012 Dinosaur tracksites of the Paluxy River Valley (Glen Rose Formation, Lower Cretaceous), Dinosaur Valley State Park, Somervell County, Texas. In *Proc. of the V Int. Symp. about Dinosaur Palaeontology and Their Environment*, vol. **41**, p. 69, Salas de los Infantes, Burgos, Spain.
54. Turner ML, Falkingham PL, Gatesy SM. 2022 What is stance phase on deformable substrates? *Integr. Comp. Biol* **62**, 1357–1368. (doi:10.1093/icb/icac009)
55. Schanz T, Lins Y, Viefhaus H, Barciaga T, Läbe S, Preuschoft H, Witzel U, Sander PM. 2013 Quantitative interpretation of tracks for determination of body mass. *PLoS One* **8**, e77606. (doi:10.1371/journal.pone.0077606)
56. Marchetti L *et al*. 2019 Defining the morphological quality of fossil footprints: problems and principles of preservation in tetrapod ichnology with examples from the Palaeozoic to the present. *Earth Sci. Rev*. **193**, 109–145. (doi:10.1016/j.earscirev.2019.04.008)
57. Falkingham PL, Gatesy SM. 2020 Discussion: Defining the morphological quality of fossil footprints: problems and principles of preservation in tetrapod ichnology with examples from the Palaeozoic to the present by Lorenzo Marchetti et al. *Earth Sci. Rev*. **208**, 103320. (doi:10.1016/j.earscirev.2020.103320)
58. Griffin BW, Prescott T, Jannel A, Falkingham PL. 2026 Supplementary material from: Penetrative track morphology and sediment parameters: subsurface layers are robust to changes in substrate properties. Figshare. (doi:10.6084/m9.figshare.c.8268142)